# Numerical Investigation of a Uniform Viscous Transonic Flow Past a Rotating Circular Cylinder

Inés Arauzo and José Miguel Pérez

## 1   Introduction

Since the inauguration of the International Space Station (ISS) in 1998, human presence in space has slowly become a common event. Nonetheless, the relaunch of the space race, with private companies such as SpaceX, Blue Origin, or Virgin Galactic as its protagonists, has recently implied a radical change when it comes to planning space missions. Furthermore, the promise of affordable space tourism in the relatively near future exposes the urgent necessity to improve the present technology and designs, being necessary for optimizing alternatives that are more convenient for the long run, in other words, reusable space vehicles. In this context, the pioneer company was SpaceX, which had put its efforts into developing reusable launchers in the last few years, reaching ten successful launches with the same booster (B1051) in 2021. However, recovering the launcher is just a fraction of the technological development needed to retrieve the full vehicle, firstly, because this stage does not leave the close atmosphere at any moment of its flight and, secondly, because this stage has enough fuel to make a controlled comeback. With this information in mind, it is quite evident that the most technologically challenging phase will be the last one, the reentry. In this phase, the ship (also called debris when it is uncontrolled) starts to decay due to the combination of gravity forces and the atmospheric-induced drag. When the vehicle reaches altitudes below 120 km over the Earth's surface, the air density becomes significant enough for the aerodynamic drag to make the ship slow down to speeds below the necessary one to orbit at that altitude (the orbital velocity). This is the starting point of the reentry trajectory.

During the reentry phase, the ship quickly falls into a much denser atmosphere, increasing the aerodynamic drag, the dynamic pressure, and the ship's surface

I. Arauzo · J. M. Pérez (✉)
Universidad Politécnica de Madrid, Madrid, Spain
e-mail: ines.arauzo.andres@alumnos.upm.es; josemiguel.perez@upm.es

temperature. These almost instantaneous changes in the flight conditions make the ship reach a huge range of speeds, going from hypersonic to subsonic, depending on the geometry and the initial conditions. For that, thermal protection systems (TPS) are needed; see Wu et al. (2007) and Abdi et al. (2018) in the case of a circular cylinder. These systems can be ablative, refractory insulation, and passive and active cooling systems. Another possibility is reducing the reentry velocity in the upper layers of the atmosphere, highlighting the retro-propulsion systems, as used by B105.

One option that could be added to the second category of techniques, but without fuel consumption, would be to increase lift at the beginning of reentry. This would reduce speed without excessive friction and heat transfer (due to the low density at high altitudes). However, since reentry vehicles are usually blunt (reentry capsules), they do not usually generate high lift. One way to achieve such lift would be through the Magnus effect, which can be achieved by rotating the reentry vehicle fuselage. In the present paper, we intend to analyze with CFD, using a simplified problem, the changes in the aerodynamics that the Magnus effect would introduce in a rotating ship. This ship is replaced in this work by a rotating circular cylinder, with a constant angular velocity defined in a two-dimensional and uniform subsonic/transonic flow. This problem has been studied in the literature primarily in the incompressible (Tokumaru & Dimotakis, 1993; Sengupta et al., 2003) or low subsonic flow regime (Teymourtash & Salimipour, 2017) but without the presence of shock waves and regions with the supersonic flow. More recent works have investigated this problem in the hypersonic regime; see John et al. (2016).

Three dimensionless parameters characterize the problem: the Reynolds number based on the diameter of the circular cylinder and the properties of the free flow $\mathrm{Re} = \frac{\rho V_\infty D}{\mu}$, the ratio between tangential velocity on the cylinder surface and that of the freestream velocity $\alpha = \frac{\omega D}{2 V_\infty}$, and the Mach number of the free flow $M_\infty = \frac{V_\infty}{\sqrt{\gamma R T_\infty}}$. Other parameters such as the Prandtl number or the ratio between specific heats will remain constant and equal to their standard values for air. The rotation implies that in some places of the cylinder's surface, the freestream velocity is in the same direction as the flow driven by the rotation. In contrast, these velocities will be opposite on the opposite side. In our case, the cylinder will rotate clockwise, so the part with the highest velocity will be the upper part of the cylinder and the part with the lowest velocity will be the lower part. This changes the pressure distribution over the cylinder surface and can generate a normal shock wave at the top (suction side).

Although the objective is to study supersonic and hypersonic flows, in this work, we are going to focus on high subsonic flows in such a way that adding the effect of rotation generates a shock wave on the suction side of the body.
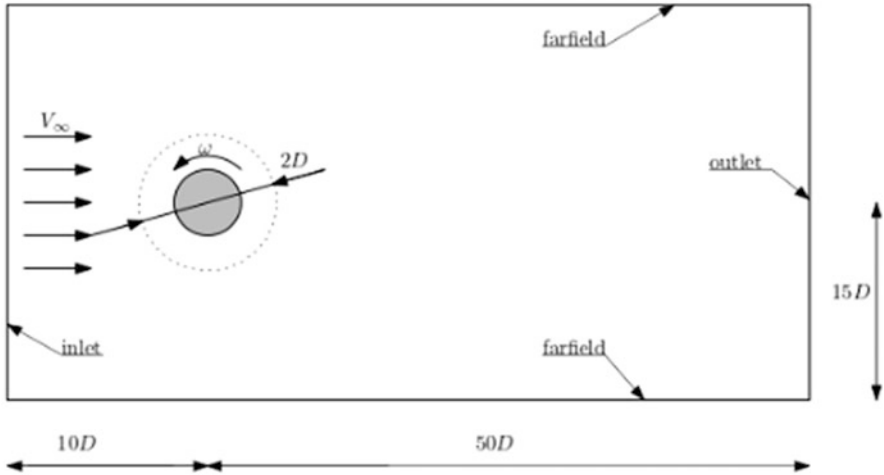
**Fig. 1** Domain and boundary conditions

## 2  Problem Definition

Figure 1 shows a sketch of the problem. This is defined by a rotating cylinder whose diameter is $D = 2R$, and its angular velocity is $\omega$. The cylinder is immersed in a flow with a freestream velocity $U_\infty$. The ratio between these two velocities is the coefficient described above, $\alpha = \frac{\omega D}{2V_\infty}$. The simulations have been performed for negative values of $\alpha$ (clockwise rotation). In order to study the dependence of the aerodynamic coefficients with the Mach number of the freestream and the nondimensional rotating speed $\alpha$, three cases will be analyzed: case A, Re = 10,000, $M_\infty = 0.5$, and $\alpha = 1$; case B, Re = 10,000, $M_\infty = 0.1$, and $\alpha = 1$; and case C, Re = 10,000, $M_\infty = 0.5$, and $\alpha = 0.1$. The circular cylinder is located at the origin of the coordinate system (see Fig. 1 for details). Concerning the boundary conditions, the value of the velocity and the values of the total pressure and temperature have been imposed in the inflow, while the static pressure has been considered in the outflow. Finally, an adiabatic no-slip boundary condition on the cylinder's surface has been used.

## 3  Numerical Simulation

For the numerical resolution of the system, the domain must be discretized with a mesh. In this case, the mesh is a structured mixture of a C-mesh in the area close to the cylinder and an H-mesh for the rest of the domain. Furthermore, stretching was implemented in the whole domain in order to capture the desired information with a

good resolution while easing the computational cost. The governing equations for the simulation are the 2D Navier-Stokes equations:

$$\frac{\partial}{\partial t}\int_{\Omega}\vec{W}d\Omega + \oint_{\partial\Omega}\overrightarrow{(F}_c - \vec{F}_v)dS = 0 \tag{1}$$

$$\vec{W} = \begin{bmatrix} \rho \\ \rho u \\ \rho v \\ \rho E \end{bmatrix}; \quad \vec{F}_c = \begin{bmatrix} \rho V \\ \rho u V + n_x p \\ \rho v V + n_y p \\ \rho H V \end{bmatrix}; \quad \vec{F}_v = \begin{bmatrix} 0 \\ n_x \tau_{xx} + n_y \tau_{xy} \\ n_x \tau_{yx} + n_y \tau_{yy} \\ n_x \Theta_x + n_y \Theta_y \end{bmatrix} \tag{2}$$

where $\Omega$ is the volume of the domain, $\partial\Omega$ is its contour, $V \equiv \vec{v} \cdot \vec{n} = n_x u + n_y v$ is the normal direction on the boundaries, $E$ is the total energy per mass unit, $\tau_{ij}$ are the components of the stress tensor, and $\Theta_x$ and $\Theta_y$ are given by $\Theta_x = u\tau_{xx} + v\tau_{xy}$ and $\Theta_y = u\tau_{yx} + v\tau_{yy}$. The method used for the temporal integration is an implicit second-order scheme accelerated with a dual time step.

## 4    Results and Discussion

As aforementioned, the aim is to study the dependence of the aerodynamic coefficients on the Mach number and $\alpha$. These results are shown in Figs. 2, 3, and 4 which show the gradient of the pressure field colored with the Mach number and the instantaneous streamlines defined by the momentum density ($\rho u, \rho v$).
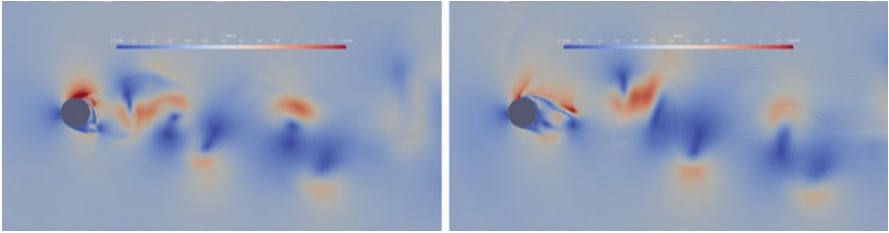


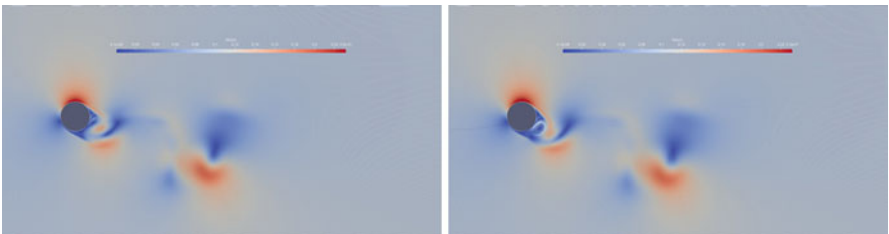**Fig. 2**  Case A: Flow past a cylinder at $M_\infty = 0.5$ and $\alpha = 1$. Maximum mach number = 1.3



**Fig. 3**  Case B: Flow past a cylinder at $M_\infty = 0.1$ and $\alpha = 1$. Maximum mach number = 0.23
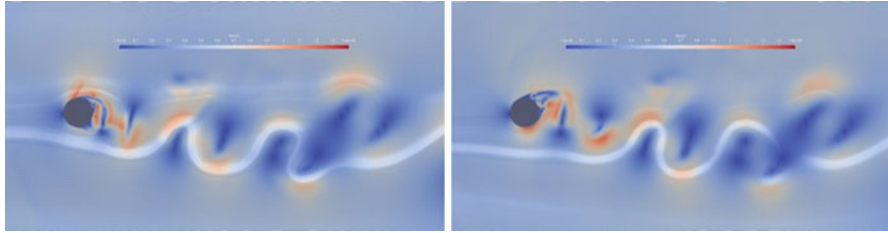
**Fig. 4** Case C: Flow past a cylinder at $M_\infty = 0.5$ and $\alpha = 0.1$. Maximum mach number $= 1.4$
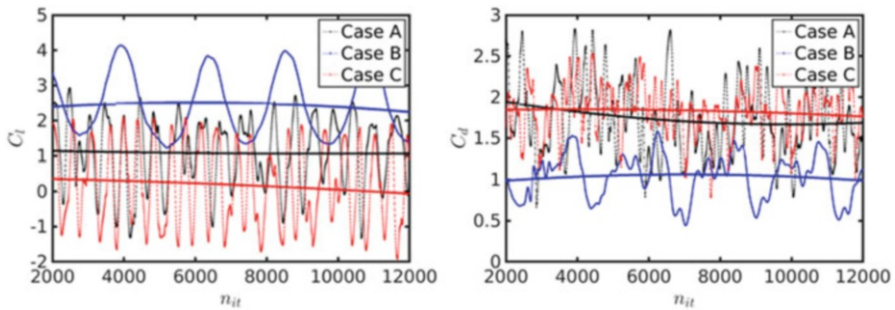


**Fig. 5** Average values of lift and drag coefficients for the three test cases as a function of the number of temporal iterations. Case A (black line), case B (blue line), and case C (red line)

**Case A (Re $=$ 10,000, $M_\infty$=0.5, and $\alpha = 1$):** Figure 2 shows two consecutive snapshots in which a shock wave can be seen on the suction side of the cylinder surface (left fig.) and how this is expelled upstream by the effect of the wake movement behind the cylinder (right fig.). The generation of this shock wave is due to the extra acceleration experienced by the fluid on the upper side induced by the cylinder rotation.

**Case B(Re=10,000, $M_\infty$=0.1, and $\alpha = 1$):** Unlike the previous case, the Mach number is lower in this case (Fig. 3). This implies that the extra acceleration due to rotation is insufficient to accelerate the flow to the supersonic regime. As in the previous case, the rotation of the cylinder induces a downward deflection of the wake.

**Case C (Re=10,000, $M_\infty$=0.5, and $\alpha = 0.1$):** This case differs from case A in the value of $\alpha$. A priori, it could be thought that the value of alpha so small is not enough to obtain a supersonic flow. However, as shown in Fig. 4, the flow is supersonic again.

Figure 5 shows the instantaneous (dot lines) and average (continuous lines) aerodynamic coefficients; $C_l = F_l / \left( \frac{1}{2\rho V_\infty^2 D} \right)$, and $C_d = F_d / \left( \frac{1}{2\rho V_\infty^2 D} \right)$ as functions on time. As seen in the first figure, $C_L$ increases when Mach decreases. This effect had already been seen previously in the literature for small Mach numbers.

Regarding the dependence with $\alpha$, $C_L$ decreases when $\alpha$ decreases. Note also that the difference between these two curves is of an order of magnitude, which agrees with the predictions made with the potential theory in which $C_L$ is proportional to the value of $\alpha$. As for the coefficient $C_D$, as can be seen, it hardly depends on the value of $\alpha$ (compare red and black curves) and decreases as the Mach number decreases.

## 5   Conclusion

This work studied the transonic flow defined on a rotating circular cylinder immersed in a transonic flow. Different simulations have been carried out, which have allowed characterizing qualitatively the behavior of the aerodynamic forces (drag and lift) as a function of the problem's parameters. We have also obtained information on the dynamics of the problem, such as the effect of the vortex shedding (wake) on the shock wave. We are presently performing different modal decomposition analyses: POD and DMD. These analyses will be completed shortly. In the case of the POD analysis, the objective is to obtain a reduced-order model that allows us to retain most of the energy of the system with the smallest possible number of modes.

## References

Abdi, R., Rezazadeh, N., & Abdi, M. (2019). Investigation of passive oscillations of flexible splitter plates attached to a circular cylinder. *Journal of Fluids and Structures, 84*, 302–317.

John, B., Gu, X., Barber, R. W., & Emerson, D. R. (2016). High-speed rarefied flow past a rotating cylinder: The inverse Magnus effect. *AIAA Journal, 54*, 16070–11680.

Sengupta, T. K., et al. (2003). Temporal flow instability for Magnus-robins effect at high rotation rates. *Journal of Fluids and Structures, 17*, 941–953.

Teymourtash, A. R., & Salimipour, S. E. (2017). Compressibility effects on the flow past a rotating cylinder. *Physics of Fluids, 29*, 016101.

Tokumaru, P. T., & Dimotakis, P. E. (1993). The lift of a cylinder executing rotary motions in a uniform flow. *Journal of Fluid Mechanics, 255*, 1–10.

Wu, C., Wang, L., & Wu, J. (2007). Suppression of the von Kármán vortex street behind a circular cylinder by a travelling wave generated by a flexible surface. *Journal of Fluid Mechanics, 574*, 365–391.